

# One-dimensional quantum chaos: Explicitly solvable cases

Yu. Dabaghian<sup>1</sup>), R. V. Jensen, R. Blümel

Department of Physics, Wesleyan University, CT 06459-0155, Middletown, USA

Submitted 9 July 2001

We present quantum graphs with remarkably regular spectral characteristics. We call them *regular quantum graphs*. Although regular quantum graphs are strongly chaotic in the classical limit, their quantum spectra are explicitly solvable in terms of periodic orbits. We present analytical solutions for the spectrum of regular quantum graphs in the form of explicit and exact periodic orbit expansions for each individual energy level.

PACS: 05.45.Mt, 03.65.Sq

Consider a point particle moving along a network of bonds and vertices. Schematically, the network is represented by a graph  $\Gamma$  (see Fig.1 for an example), which

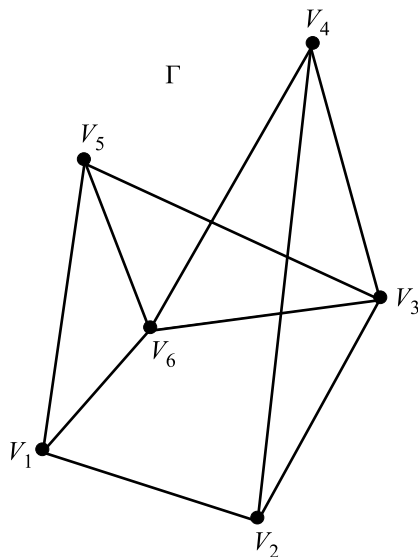


Fig.1. A generic (quantum) graph with five vertices and six bonds

consists of  $N_B$  bonds and  $N_V$  vertices. The vertices are denoted by  $V_i$ ; a bond connecting vertices  $i$  and  $j$  is denoted by  $B_{ij}$ . The set of bonds and vertices of  $\Gamma$  defines its *geometry*. We define a set of the bond potentials,  $U_{ij}(k, x)$ , where  $x$  and  $k$  are correspondingly the coordinate and the momentum of the particle on the bond  $B_{ij}$ . The vertices of  $\Gamma$  may be equipped with  $\delta$ -sources, etc. The geometry of  $\Gamma$  does not uniquely define the dynamics of a particle on  $\Gamma$ . In fact, since for any given geometry the graph may be “dressed” with arbitrary bond and vertex potentials, there exist infinitely many “dynamical realizations” of  $\Gamma$ . We call the set of bond and vertex potentials the “dynamical dressing” of the graph.

Previously [1–5], mainly the “bare-bond” graphs were studied, where the particle moves freely on the bonds.

In this paper we focus on cases that have no turning points on the bonds, i.e. the energy of the particle is larger than all of the bond potentials,  $E > U_{ij}(x, k)$ ,  $x \in B_{ij}$ . A simple way to implement this condition is to require that the system is *scaling* [6–10]. This implies  $U_{ij}(x, k) = \lambda_{ij}(x) k^2$ , where the functions  $\lambda_{ij}(x)$  are bounded for all  $x$ . In this paper we consider only simple cases where the functions  $\lambda_{ij}(x)$  are  $x$  independent constants,

$$U_{ij}(x, k) = \lambda_{ij} k^2. \quad (1)$$

This is very similar to moving on a free graph except for substituting the bond lengths with the action lengths

$$S_{ij}^0 = \beta_{ij} L_{ij}, \quad (2)$$

where  $L_{ij}$  is the length of the bond  $B_{ij}$ , and  $\beta_{ij} = \sqrt{1 - \lambda_{ij}}$ . The scaling assumption (1) is not an oversimplification of the problem. Plenty of room is left for very interesting phenomena. Moreover, scaling quantum systems of this kind are the analogues of certain electromagnetic ray-splitting systems which have already been investigated experimentally in the laboratory [7–9].

For all but the most trivial graphs, i.e. linear or circular graphs with vanishing bond and vertex potentials, the classical motion on a graph, independently of any particular dressing, is fully chaotic with positive topological entropy [11]. This means that the number of possible periodic orbits traced by the particle increases exponentially with their lengths. If no dynamical turning points are present, the topological entropy is independent of the dynamical dressing and depends only on the geometry of the graph. Since at any vertex different from a “dead-end” vertex the classical particle has to choose randomly between several possibilities (reflection, transmission, branching), the particle’s dynamical evolution resembles a stochastic, Markovian process.

<sup>1</sup>)e-mail: ydabaghian@wesleyan.edu

Given their classical chaoticity it is surprising that the density of states of quantum graphs can be obtained exactly in terms of periodic orbit expansion series [1, 3–5]. Furthermore, quantum graphs are considerably “more integrable” than all the previously known exactly solvable quantum systems. For example we will show below that for a certain class of quantum graphs – we call them *regular quantum graphs* – there exists an explicit and exact periodic orbit expansion for every quantum energy level. In other words, although the classical limit of regular quantum graphs is chaotic, each individual level of their spectra can be obtained exactly and explicitly via an analytical formula containing an explicit sum over the periodic orbits of the graph. To the authors’ knowledge this is the first time that the spectrum of a quantum chaotic system is obtained both *exactly* and *explicitly*.

The formal definition of regular quantum graphs is based on the properties of the spectral equation [3–5]

$$\det[1 - S(k)] = 0, \quad (3)$$

where  $S(k)$  is the scattering matrix of the graph [3]. The modulus of the complex function (3) is a trigonometric polynomial of the form

$$\cos(S_0 k - \pi \gamma_0) - \Phi(k) = 0, \quad (4)$$

where

$$\Phi(k) = \sum_i a_i \cos(S_i k - \pi \gamma_i) \quad (5)$$

and

$$S_0 = \frac{1}{k} \sum_{i < j} \int_{B_{ij}} k_{ij}(x) dx \quad (6)$$

is the total reduced action length of the graph  $\Gamma$  and the constant frequencies  $S_i < S_0$  naturally emerge as combinations of the reduced classical actions (2). Under the scaling assumption, the coefficients  $a_i$ ,  $\gamma_0$  and  $\gamma_i$  are constants.

We now define regular quantum graphs. They satisfy

$$\alpha = \sum_i |a_i| < 1. \quad (7)$$

The motivation for this definition is the following: it allows us to solve (4) formally for the momentum eigenvalues  $k_n$ ,

$$k_n = \frac{\pi}{S_0} [n + \mu + \gamma_0] + \frac{1}{S_0} \begin{cases} \arccos(\Phi(k_n)), & \text{for } n + \mu \text{ even} \\ \pi - \arccos(\Phi(k_n)), & \text{for } n + \mu \text{ odd} \end{cases}, \quad (8)$$

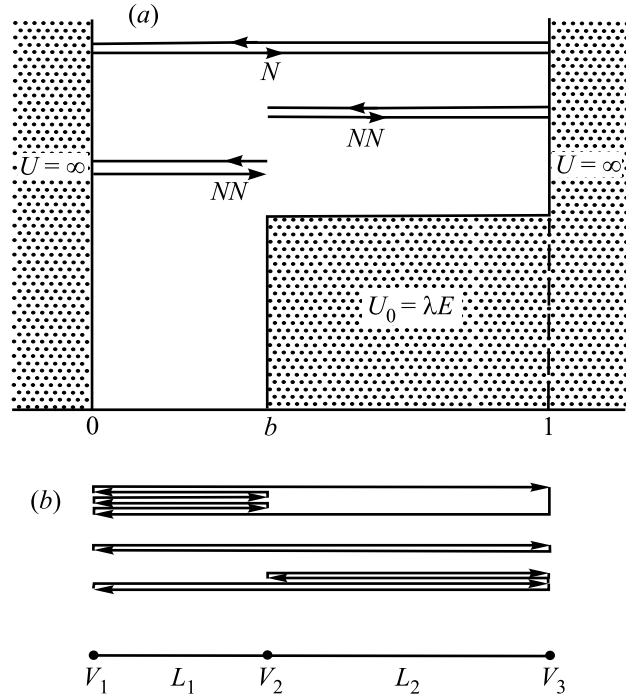


Fig.2. (a) Simple step potential, a basic problem in one-dimensional quantum mechanics. Also shown are examples of Newtonian  $N$  and non-Newtonian ( $NN$ ) periodic orbits used in the periodic orbit expansion of its energy eigenvalues (see Text). (b) Three-vertex hydra graph corresponding to the step potential above

where  $\mu$  is a fixed integer chosen such that  $k_1$  is the first non-negative solution of (4). Because of (7) the second term of (8) assumes only values between  $u$  and  $\pi/S_0 - u$ , where  $0 < u = \arccos(\alpha)/S_0 < \pi/2S_0$ . Thus, for regular graphs, the points

$$\bar{k}_n = \frac{\pi}{S_0} (n + \gamma), \quad n = 1, 2, \dots, \quad \gamma \equiv \mu + \gamma_0 \quad (9)$$

are guaranteed not to be roots of (3) and serve as separators between roots number  $n$  and  $n+1$ . Obviously the function (9) reflects the average behavior of the levels of the momentum. It is simply the inverted average staircase case,  $\bar{k}_N = \bar{N}(k)^{-1}$ . Geometrically the points (9) are the intersection points between the staircase function,  $N(k) \equiv \sum_n \Theta(k - k_n)$ , and the average staircase  $\bar{N}(\bar{k})$  resulting in the crossing condition

$$\bar{N}(\bar{k}_n) = N(\bar{k}_n) = n. \quad (10)$$

The crossing condition (10) is illustrated in Fig.3.

The existence of the separating points (9) implies that the roots (8) are confined to the “root zones”, or “root intervals”  $I_n = [\bar{k}_{n-1}, \bar{k}_n]$ ,  $n = 1, 2, \dots$ . If  $\alpha \leq C < 1$  holds ( $C$  constant), equation (8) implies the existence of finite-width root-free “forbidden zones”

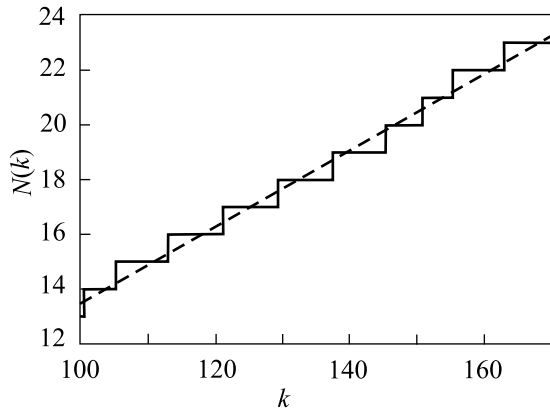


Fig.3. The staircase function  $N(k)$  and the average staircase  $\bar{N}(k)$ . For the regular graphs the average staircase intersects every “stair” of the  $N(k)$  graph, with the separators (9) showing as the intersection points  $N(\bar{k}_n) = \bar{N}(\bar{k}_n)$

$R_n = (\bar{k}_n - u, \bar{k}_n + u)$  surrounding every separating point  $\bar{k}_n$ , where no roots of (3) can be found. The roots of (3) can only be found in the “allowed zones”  $Z_n = [\bar{k}_{n-1} + u, \bar{k}_n - u]$ , which are subsets of the root intervals  $I_n = [\bar{k}_{n-1}, \bar{k}_n]$ . For  $C \rightarrow 1$  the width of the forbidden regions shrinks,  $u \rightarrow 0$ , and the allowed zones occupy the whole interval,  $Z_n \rightarrow I_n$ .

Since  $S_0$  is the largest action in (4) and (5), it can be shown [12] that  $k_n$  is the *only* root in  $Z_n$ . Therefore there is exactly one root  $k_n$  inside of  $Z_n \subset I_n$ , and this root is bounded away from the separating points  $\bar{k}_{n-1}$  and  $\bar{k}_n$  by a finite interval of length  $2u$ .

The existence of the separating points (9) and the root-free zones  $R_n$  are the key for obtaining an explicit and exact periodic orbit expansion for every root of (3). The starting point for obtaining the explicit expressions is the exact periodic orbit expansion for the density of states,  $\rho(k) \equiv \sum_{j=1}^{\infty} \delta(k - k_j)$ . As shown in [1, 3–5] it can be written explicitly as

$$\rho(k) = \bar{\rho}(k) + \frac{1}{\pi} \operatorname{Re} \sum_p S_p^0 \sum_{\nu=1}^{\infty} A_p^\nu e^{i\nu S_p^0 k}. \quad (11)$$

Here  $\bar{\rho}(k)$  is the average density of states,  $\nu$  is the repetition index, and  $S_p^0$ ,  $A_p$  are correspondingly the reduced action and the weight factor of the prime periodic orbit labeled by  $p$ . In the scaling case,  $S_p^0$  and  $A_p$  are  $k$ -independent constants [12]. Multiplying the density of states by  $k$  and integrating from  $\bar{k}_{n-1}$  to  $\bar{k}_n$  yields the value of the root contained between these separating points,

$$\int_{\bar{k}_{n-1}}^{\bar{k}_n} \rho(k) k dk = \int_{\bar{k}_{n-1}}^{\bar{k}_n} \sum_{j=1}^{\infty} \delta(k - k_j) k dk = k_n. \quad (12)$$

Performing the same procedure using the series expansion representation (11) and the crossing condition (10), we obtain

$$k_n = \frac{\pi}{S_0} n - \frac{2}{\pi} \sum_p \frac{1}{S_p^0} \sum_{\nu=1}^{\infty} \frac{A_p^\nu}{\nu^2} \sin\left(\frac{\pi}{2} \nu \omega_p\right) \sin(\pi \nu \omega_p n), \quad (13)$$

where  $\omega_p = S_p^0/S_0$ , and the  $A_p$ 's are assumed to be real (no vertex potentials).

Since all of the quantities on the right-hand side of (13) are known, this formula provides an explicit representation of the roots  $k_n$  of the spectral equation (3) in terms of the geometric and dynamical characteristics of the graph. To our knowledge, this is the first time that the energy levels of a chaotic system are expressed explicitly in terms of a periodic orbit expansion. Previously, explicit formulae for individual energy levels were known only for integrable systems. In the context of periodic orbit theory, the energy levels of integrable systems are given by the Einstein-Brillouin-Keller (EBK) formula [11]. However, apart from a few exceptional cases [13] EBK quantization is only of semiclassical accuracy.

The difference between (11) and (13) is profound. The density of states (11) allows the computation of spectral points only indirectly as the singularities of (11). Formula (13), on the other hand, allows the computation of every quantum level *individually, explicitly and exactly* in terms of classical parameters.

In order to demonstrate that the class of regular quantum graphs is not empty we present an explicit example: the one-dimensional scaled step potential with  $V_0 = \lambda E$ . A sketch of this potential is shown in Fig.3. Physically this potential is realized, e.g., by a rectangular microwave cavity partially loaded with a dielectric substance [7–9]. The scaling step potential is equivalent to the scaling three-vertex linear graph shown in Fig.2b. It has two bonds  $L_1 = b$  and  $L_2 = \beta(1 - b)$ ; the single scaling constant  $\beta$  (see (2)) is given by  $\beta = \sqrt{1 - \lambda}$ . The spectral equation is given by

$$|\det [1 - S(k)]| = \sin(Lk) - r \sin[(L_1 - L_2)k] = 0, \quad (14)$$

where  $L = L_1 + L_2$ , and  $r = (1 - \beta)/(1 + \beta)$  is the reflection coefficient at the vertex  $V_2$  between the two bonds. It defines the eigenvalues  $k_n$  only implicitly and

is usually solved by graphical or numerical methods. Application of (13), however, solves (14) explicitly in terms of periodic orbits such as the ones shown in Fig.2. In order to apply (14) we need the coefficients  $A_p$ . They are given by [10, 12]

$$A_p = (-1)^{\chi(p)} r^{\sigma(p)} (1 - r^2)^{\tau(p)/2}, \quad (15)$$

where  $r$  is the reflection coefficient at the middle vertex and  $\sigma(p)$  and  $\tau(p)$  are correspondingly the number of the reflections and the transmissions through it. Since the reflection coefficient may be positive or negative depending on whether the particle scatters from the right or from the left, the factor  $(-1)^{\chi(p)}$  is needed to keep track of how many times it appears with a minus sign, including the sign changes due to the wall ( $x = 0$  and  $x = 1$ ) reflections.

In order to illustrate the convergence of (13) we computed  $k_1$ ,  $k_{10}$  and  $k_{100}$  of the scaling step potential including periodic orbits of increasing binary length  $q$ . For the parameters of the potential we chose  $b = 0.3$  (see Fig.2) and  $\lambda = 1/2$ . Fig.4 shows the relative er-

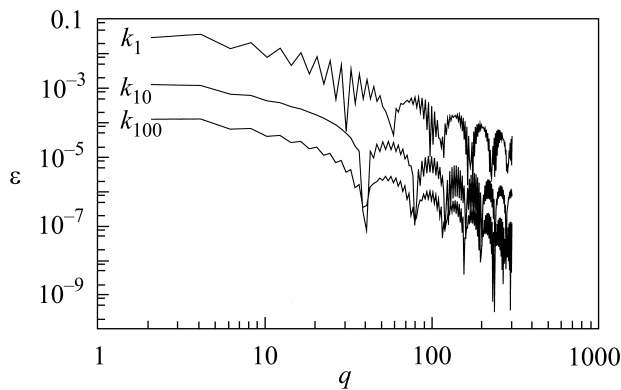


Fig.4. Relative error  $\epsilon_n^{(q)} = |k_n^{(q)} - k_n^{(\text{exact})}|/k_n^{(\text{exact})}$  of (13) (see text) by including periodic orbits up to length  $q$ . The three curves shown correspond to  $k_1$ ,  $k_{10}$  and  $k_{100}$  as indicated in the figure

ror  $\epsilon_n^{(q)} = |k_n^{(q)} - k_n^{\text{exact}}|/k_n^{\text{exact}}$  for  $n = 1, 10, 100$  and  $q$  ranging from 1 to 150. We see that even for small  $q$  the relative error is very small, decreasing further for large  $q$  as a power-law in  $q$ . The power of convergence appears to be the same for all three  $k$  and is close to  $-2$ . The convergence with  $q$  is an important result. It indicates that although (13) is only conditionally convergent it (i) converges to the correct result and (ii) is not just asymptotically convergent, but keeps converging when more and more periodic orbits are included.

Additional examples of regular quantum graphs are provided by all linear and circular quantum graphs with at most two bonds per vertex, independently of the num-

ber of vertices. In other words, for any simply connected quantum graph and any dynamical dressing there always exists a set of scaling constants  $\lambda_{ij}$  of finite measure such that the regularity condition (7) is fulfilled. Well-known particular cases of these simply connected quantum graphs are the “Manhattan potentials”, which are obvious generalizations of the simple step potential shown in Fig.2a to arbitrarily many steps inside of the well, and linear chain graphs with scaling  $\delta$  function potentials at the vertices.

It should be emphasized that the “inverse staircase expansion” (13) is not just a curious finding, valid for some simple 1D systems such as quantum graphs. Similar explicit series may be obtained for more complicated higher dimensional systems when the following two key ingredients are available. The first ingredient is the exact series expansion of the density of states (11), which has already been established for other classically chaotic systems such as, e.g., quantum billiards [14]. The second ingredient is a (piercing) average staircase function  $\bar{N}(k)$  or the inverted staircase function  $\bar{k}_n$  which intersects every stair of the staircase,  $\bar{N}(\bar{k}_n) = N(\bar{k}_n) = n$ ,  $n = 1, 2, \dots$ . The intersection points  $\bar{k}_n$  then serve as the separators for the possible root locations, and the procedure outlined in the text can be used to find the periodic orbit expansions for individual roots of the system at hand. In most cases, of course, it is highly non-trivial to obtain these two necessary ingredients. The quantum graphs themselves are an excellent illustration of this point. While the expansion (11) is valid for all quantum graphs, it is the crossing condition (10) that is violated when the inequality (7) brakes down. The regular graphs are precisely those for which the line  $\bar{N}(k) = S_0 k/\pi + \gamma$  satisfies (10) and allows the application of the analytical procedure that resulted in the explicit formula (13) for the representation and computation of individual eigenvalues  $k_n$ .

Y.D. and R.B. gratefully acknowledge financial support by NSF grants # PHY-9900730 and PHY-9984075; Y.D. and R.J. by NSF grant # PHY-9900746.

1. J.-P. Roth, in *Lecture Notes in Mathematics: Théorie du Potentiel*, Vol. 1096, Eds. A. Dold and B. Eckmann, Springer, Berlin, 1984, pp. 521–539.
2. E. Akkermans, A. Comtet, J. Desbois et al., LANL archive cond-mat/9911183.
3. T. Kottos and U. Smilansky, *Phys. Rev. Lett.* **79**, 4794 (1997).
4. T. Kottos and U. Smilansky, *Ann. Phys.* **274**, 76 (1999).
5. H. Schanz and U. Smilansky, *Phys. Rev. Lett.* **84**, 1427 (2000).

6. R.E. Prange, E. Ott, T. M. Antonsen et al., Phys. Rev. **E53**, 207 (1996).
7. L. Sirko, P. M. Koch, and R. Blümel, Phys. Rev. Lett. **78**, 2940 (1997).
8. Sz. Bauch, A. Błędowski, L. Sirko et al., Phys. Rev. **E57**, 304 (1998).
9. R. Blümel, P. M. Koch, and L. Sirko, Found. Phys. **31**, 269 (2001).
10. Y. Dabaghian, R. V. Jensen, and R. Blümel, Phys. Rev. **E63**, 066201 (2001).
11. M. Gutzwiller, *Chaos in Classical and Quantum Mechanics*, Springer, New York, 1990.
12. Y. Dabaghian, R. V. Jensen, and R. Blümel, in preparation.
13. R. I. Szabo, *Equivariant Localization of Path Integrals*, LANL archive, hep-th/9608068 (1996).
14. K. G. Anderson and R. B. Melrose, Inv. Math. **41**, 197 (1977).